Adiabatic density surface, neutral density surface, potential density surface, and mixing path[*]

HUANG Rui-xin

Department of Physical Oceanography, Woods Hole Oceanographic Institution, Woods Hole, MA 02543, USA

Abstract: In this paper, adiabatic density surface, neutral density surface and potential density surface are compared. The adiabatic density surface is defined as the surface on which a water parcel can move adiabatically, without changing its potential temperature and salinity. For a water parcel taken at a given station and pressure level, the corresponding adiabatic density surface can be determined through simple calculations. This family of surface is neutrally buoyant in the world ocean, and different from other surfaces that are not truly neutrally buoyant. In order to explore mixing path in the ocean, a mixing ratio m is introduced, which is defined as the portion of potential temperature and salinity of a water parcel that has exchanged with the environment during a segment of migration in the ocean. Two extreme situations of mixing path in the ocean are $m=0$ (no mixing), which is represented by the adiabatic density curve, and $m=1$, where the original information is completely lost through mixing. The latter is represented by the neutral density curve. The reality lies in between, namely, $0<m<1$. In the turbulent ocean, there are potentially infinite mixing paths, some of which may be identified by using different tracers (or their combinations) and different mixing criteria. Searching for mixing paths in the real ocean presents a great challenge for further research.

Key words: adiabatic density surface, neutral density surface, potential density surface, mixing path

CLC number: P731   **Document code:** A   **Serial number:** 1009-5470(2014)04-0001-19

Water mass analysis, including its spreading and transformation, has been a classical topic in physical oceanography. For example, the core layer method was widely used in many classical papers, such as Wust (1935); a more concise description can be found in Stewart (2009). As an improvement, different surfaces were introduced for analyzing the lateral distribution of water properties. A landmark was the pioneering work of Montgomery (1938) on isentropic analysis. Since then many attempts have been made to find suitable surfaces for isentropic (or adiabatic, i.e. without changing potential temperature and salinity) motions, such as the potential temperature surface and the isopycnal surface (including the potential density surface and different types of approximately neutral density surfaces). The essential criteria/goals in searching for suitable surfaces for water mass analysis are as follows.

1) Finding the trajectories/surfaces along which a water parcel can travel adiabatically and net-buoyancy-freely.

2) Finding the surfaces on which two water parcels can adiabatically exchange their horizontal positions and without changing the shape of the original surface.

3) Finding the mixing trajectories or mixing surfaces.

The mixing path is the trajectory of a water mass spreading/ transforming in the ocean. In the turbulent ocean, this is a loosely defined term. By definition, it is a Lagrangian trajectory along which certain water properties are conserved. In addition, mixing takes place along the trajectory, leading to a gradual modification of water properties. As a result, the trajectory of a Lagrangian float may be different

from the trajectory of a water mass because the former involves no mixing, but the latter involves mixing.

A mixing surface is a generalization of mixing path, and it is defined as the surface on which a water parcel can move around, spreading and mixing with the environment. Movement of a water parcel on the mixing surface is always involved with a gradual modification of its properties.

The specific entropy of seawater is closely linked to its potential temperature (Feistel, 2003, 2005). Water parcels continuously change their entropy due to lateral and vertical diffusion. Thus, constant entropy surfaces diagnosed from the ocean cannot be used as the surfaces for analyzing a water mass's movement in the ocean.

Montgomery's (1938) analysis was based on the σ_t surface. By definition, $\sigma_t = \rho(S, T, p=0)$ (where ρ is density, S is salinity, T is temperature, and p is pressure) is not a conserved quantity, so this does not lead to an isentropic surface. As a better alternative, the potential density surface (PDS hereafter) $\sigma_p = \rho(\Theta, S, p_r) = \text{const.}$ (where Θ is potential temperature, p_r is reference pressure) was introduced and widely used in hydrographic data analysis. However, the PDS is not perfect either, because at depths away from the reference pressure, potential density cannot accurately represent the local stratification. In fact, stratification or static stability is defined using the local pressure as reference. Due to the nonlinearity of the equation of the state, using a non-local reference pressure to calculate the static stability can lead to a value quite different from the truth. To overcome this problem, the patched potential density method was introduced, e.g. Reid (1994) or de Szoeke, et al (2005).

As an improvement, the neutral density surface (NDS hereafter) was introduced. The basic concept of a NDS was to build up a surface whose tangent at each point matches the local potential density surface tangent, as first postulated by Forster, et al (1976); their idea has been generalized into a theory of neutral density and NDS, e.g., McDougall (1987a), Jackett, et al (1997).

Due to the nonlinearity of equation of state, the helicity of seawater is non-zero. (Helicity for a vector A is defined as $H = A \cdot \nabla \times A$. For the application to the NDS, $A = \rho(\beta \nabla S - \alpha \nabla \Theta)$ (where β is the haline constraction coefficient, and α is the thermal expansion coefficient) is the neutral vector, see Jackett, et al, 1997). Thus, a NDS may depend on the paths chosen in defining it. As a result, an exact three-dimensional neutral surface does not exist in the ocean (McDougall, 1987a). In addition to the approximate NDS algorithm postulated by Jackett and McDougall (1997), there are other ways to define an approximate NDS, such as the minimization technique postulated by Eden, et al (1999), or the orthobaric density surface by de Szoeke, et al (2009).

However, on any 2-D (two-dimensional) vertical plane the situation is different. On a 2-D surface, the slope of the potential density surface (using the local pressure as the reference) is a 2-D vector field. If the stratification is stable, the local isopycnal slope cannot be vertical. Thus, from this 2-D vector field, a family of neutral curves can be constructed. For example, one can use the simple Euler method or any similar, more accurate, method. This family of curve has the following properties. First, everywhere the tangent of these neutral curves matches the tangent of the local potential density surface. Second, through any given point on this 2-D surface, there is only one neutral curve.

Although the neutral density and the NDS are now often used in oceanographic data analysis, some of their fundamental properties have not yet been examined thoroughly. In particular, it is not clear whether a water parcel moving on a NDS will always have the same in-situ density as the local water parcel originally sitting on the surface. In fact, whether the so-called NDS is really neutrally buoyant has not been rigorously proven.

There is another type of density surface, first discussed by McDougall (1987b) in connection with the propagation of the Submesoscale Coherent Vorticies (SCV). In this study, we will call this surface the adiabatic density surface (ADS hereafter) and will show that a water parcel can adiabatically

travel on its ADS and net-buoyancy-freely, i.e., that it satisfies the first of the above criteria.

Unfortunately, due to thermobaricity, there is no surface in the ocean along which two water parcels can exchange their horizontal positions through adiabatic motions without changing the shape of the corresponding surface. This can be shown as follows.

Assume that on a thermodynamic surface (a PDS, a quasi-NDS or any other similar surface) there are two water parcels A and B with unit mass, sitting on pressure levels ρ_A and ρ_B, $\Delta\rho=\rho_A-\rho_B >0$. If we adiabatically move parcel A to the position of B, its in-situ density change is

$$\Delta\rho_{A\to B} = \rho_A(B) - \rho_A(A) \simeq \rho_0 \Delta p \kappa_\eta(A),$$

where $\rho_A(A)$ and $\rho_A(B)$ depict water parcel A's density at location A and B, ρ_0 is the reference density, Δp is the pressure difference, and $k_\eta(A)$ is the compressibility of seawater for parcel A. Similarly, if we move parcel B to point A, its in-situ density change is

$$\Delta\rho_{B\to A} = \rho_B(A) - \rho_B(B) \simeq -\rho_0 \Delta p \kappa_\eta(B).$$

The net density change of the system is

$$\Delta\rho_{A,B} \simeq \rho_0 \Delta p \left[\kappa_\eta(A) - \kappa_\eta(B)\right].$$

Due to thermobaricity, the net density change is non-zero in general. As a result, exchanging the positions of two water parcels on any surface must lead to a change in the density structure of the system, unless other non-adiabatic processes are involved. Of course, there are some trivial exceptional cases when these two parcels sit on the same pressure level, or they have the same compressibility.

We will examine the properties of the ADS and its relation with the PDS in detail. However, neither the NDS nor the ADS can accurately represent the processes relating to mixing in the oceans. In particular, although the NDS can be used to describe mixing in the vicinity of each station, as soon as water parcels are mixed, they will leave the NDS and sink to a deeper level because of cabbeling. Thus, the NDS does not represent the mixing trajectories.

One of the primary means of water mass transport/spreading is due to a fast, sometime well-organized, current, such as a deep western boundary current stemming from a site of deep water formation. The other means is through turbulent diffusion, which is closely linked to mesoscale and submesoscale eddies. A good example is the spreading of the Mediterranean Overflow Water (MOF) in the North Atlantic. The tongue-like feature of MOF has been known for a long time, but there is no permanent current associated with it. In fact, the spreading of MOF is primarily due to the westward propagating mesoscale eddies, called Meddies, e.g., Armi, et al (1989).

Another example is AABW (Antarctic Bottom Water), which influences properties as far as into the Northern Hemisphere. Wijffels, et al (1996) analyzed water masses and circulation at 10°N in the Pacific, and they were able to identify a substantial contribution of bottom water having Antarctic origin. Schmitz, et al (1993) analyzed water masses and circulation in the North Atlantic; they examined the Atlantic component of the global conveyor belt and they were able to trace the influence of AABW as far as 30°~40°N.

Recent studies indicate that even the first type of current-related spreading may contain a substantial contribution due to eddies. For example, Lozier (2010) summarized the alternative paths of the Conveyor Belt in the world ocean. It appeared that eddies shed from the deep western boundary current can transport a substantial portion of the newly formed deep water in the North Atlantic Ocean, and thus can make up an alternative pathway for the meridional overturning circulation.

The mixing path and mixing surface are essentially defined as the result of tracing certain physical properties of water masses. The ocean is a turbulent environment. Although we may be able to define the mixing path or mixing surface based on a single realization, it may not be a truthful representation of the ocean circulation. On the other hand, large-scale features identified from a hydrographic database are some kind of (incomplete) ensemble mean of the ocean state.

Water mass analysis, including the generation and transformation of water masses, has been the backbone of classical physical oceanography. A main focus is to identify the origin and pathway of

water masses. In many classical studies, tongue-like features associated with different tracers, such as potential temperature, salinity and oxygen, have been used as clues. Apparently, many types of tracer can be used in searching the mixing paths; however, the multiplicity of mixing paths has not received due attention. As the study of oceanography enters the era of eddy-resolving oceans, the multiplicity of potential mixing paths becomes an obvious issue, e.g. Lozier (2010); thus, in this study, we will emphasize such a possibility.

The primarily goals for this study are as follows. First, we will identify a family of surfaces, along which a water parcel can move adiabatically and net-buoyancy-freely; in addition, we will show that the so-called NDS currently used in the community is not really neutral.

Second, the intrinsic properties of the PDS, ADS and NDS are compared in detail. As shown above, there is no surface in the ocean on which two water parcels can exchange their positions without changing the environment (such as its entropy or gravitational potential energy).

Third, we explore the possibility of defining the mixing path or mixing surfaces in the ocean. The ocean is a turbulent environment and there are two ways to find ensemble mean paths:

The first way is searching for mixing paths based on ocean states at different time periods. One can calculate mixing paths based on numerical simulations of the world ocean circulation; alternatively, one can find such mixing paths using the Monte Carlo method.

The second way is using climatological mean hydrographic data, such as WOA01 (Conkright, et al, 2002) to infer the mixing paths. (The WOA01 data are formulated in terms of z-level coordinate. This is converted into a dataset in the pressure coordinate for the analysis in this study.) The WOA01 can be treated as an (incomplete) ensemble mean of water property distribution. Due to limitations in data collection, databases like WOA01 are definitely not perfect because the ocean is under-sampled and observations have considerable errors. In addition, there are large signals due to isopycnal heaving, eddy activity and climate

variability. Nevertheless, these databases provide us the best available information about the ocean state and its variability over the past decades. Thus, mixing paths inferred from such a climatological dataset may best represent the mixing paths in the actual world ocean.

This study is organized as follows. In Section 2, the definition of ADS is introduced. In Section 3, the PDS and NDS, plus their relation with the ADS, are discussed. The similarities and differences of these surfaces are discussed in Section 4. The multiplicity of ADSs is discussed in Section 5. Searching for the mixing paths in the ocean has been an important topic, and we begin the discussion in Section 6, using the classical case of AABW formation as an example. The reexamination of potential mixing paths reveals the complicated situation in the ocean, as discussed in Section 7. In fact, due to the chaotic nature of turbulent flow and eddy motions, the number of potential mixing paths is infinite, and a mixing ratio is introduced as a tool to identify potential mixing paths in the ocean. As will be discussed in Section 8, the estimate of the mixing ratio in the ocean is a great challenge. Finally, we conclude in Section 9.

1 Adiabatic density surface

The ADS is defined as the surface along which a water mass can move adiabatically, i.e., with no change in potential temperature and salinity. McDougall (1987b) postulated a differential relationship for such a surface; he explored its properties in a model ocean with a linear equation of state and discussed the relation between such a surface and the PDS.

The differential relationship for an ADS is inconvenient for application, and a simpler way is to define it by solving a nonlinear equation. Assume that a given water parcel moves adiabatically, without changing its potential temperature Θ_0 and salinity S_0. Anywhere in the world ocean, its *in-situ* density is a function of the *in situ* pressure, $\rho=\rho(\Theta_0, S_0, p)$. On the other hand, taking a water column at any station (λ, θ) (λ is the longitude and θ is the latitude) in the world ocean, the *in-situ* density is a

function of the *in-situ* pressure $\rho=\rho[\Theta(\lambda, \theta, p, t), S(\lambda, \theta, p, t), p]$, where t is the time, $\Theta(\lambda, \theta, p, t)$, $S(\lambda, \theta, p, t)$ are given functions at this station and need not equal Θ_0, S_0. For large-scale or meso-scale problems, the *in-situ* density monotonically increases with pressure. These two density functions constitute a nonlinear equation for a single unknown p,

$$\rho(\Theta_0, S_0, p)=\rho[\Theta(\lambda, \theta, p, t), S(\lambda, \theta, p, t), p] \quad (1)$$

In general, there is a solution of this equation. [Eq. (1) may have multiple solutions, i.e. an ADS can have multiple sheets/branches, as will be discussed shortly]. Connecting these depths (pressures) in the world ocean gives the ADS (denoted as σ_a hereafter). If this equation has no solution at a station, the ADS either outcrops or grounds. According to Eq. (1), an ADS is a two-variable (Θ_0, S_0) function; thus, an ADS cannot be represented by assigning a single value, such as a density. By definition, the ADS has the following characteristics:

First, it is defined point by point in the world ocean, so it is not path-dependent. This is in contrast to the commonly used NDS, which is defined by following certain paths step by step.

Second, the depth of an ADS is not constant. Since the water parcel conserves its original properties, thus, under different pressure, the corresponding *in situ* density at different locations on an ADS is not constant.

Third, an ADS applies to cases in hydrostatic equilibrium; thus, it can be used for the cases of ageostrophic and time-dependent flows, in particular for the cases involved with meso-scale eddies. The potential temperature and salinity profiles $\Theta(\lambda, \theta, p, t)$, $S(\lambda, \theta, p, t)$, at a station may vary with time; thus, the ADS for a given parcel can be time-dependent.

Fourth, each water parcel has its own ADS. In general, the ADSs for different water parcels are different, although they may intersect each other. When a water parcel moves to some other points on its ADS, it has the same *in situ* density as the local water parcel; but these two parcels may have different potential temperature and salinity; thus, they belong to different ADSs and hence cannot exchange their positions through adiabatic movements on this ADS, i.e. watermass positions on an ADS are non-exchangeable.

2   The potential density surface and the neutral density surface

2.1   The potential density surface and its link to the adiabatic density surface

The PDS is defined as follows: First, a reference pressure is chosen and used to calculate the corresponding potential density value for all grid points in the ocean. Second, a PDS consists of all points having the same potential density value, which is equal to the *in situ* density only at the reference pressure. It is well-known that the PDS may have multiple sheets, or reversion.

The ADS and the PDS constitute a pair of dual surfaces in the ocean. For a given station and depth, a pair of these surfaces pass through it. An important characteristic of the ADS is that the original water parcel O can travel to any point on this surface, such as points A and B in Fig. 1a. By definition, when parcel O travels to points A and B, it has the same *in situ* density as parcels originally sitting in A or B; therefore, such a movement is truly buoyancy-free. In contrast, the commonly used neutral surface is not exactly buoyancy-free.
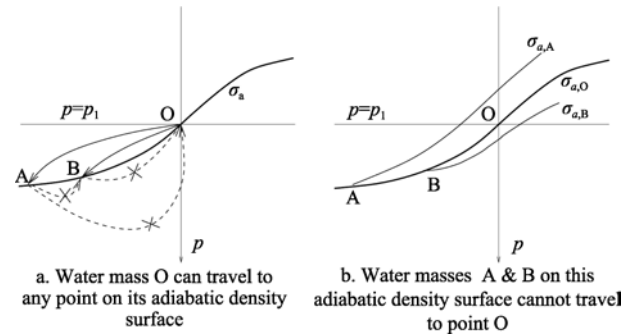

a. Water mass O can travel to   b. Water masses A & B on this
any point on its adiabatic density   adiabatic density surface cannot travel
surface   to point O

Fig. 1   The property of the ADS. The dashed lines with arrows and crosses in (a) indicate forbidden paths; $\sigma_{a, O}$, $\sigma_{a, A}$ and $\sigma_{a, B}$ in (b) indicate the ADS starting from point O, A and B, respectively. See the main text for detailed discussion

Although water parcels A and B sit on this surface, they have different potential temperature and salinity; they cannot interchange their positions on this surface. If we exchange their horizontal positions, they may leave this surface. In addition, they cannot travel to point O adiabatically without leaving this ADS. These forbidden movements are indicated by the small crosses in Fig. 1a. As shown in the introduction, if two water parcels have different

potential temperature and salinity, their compressibility is different. Thus, the same pressure change can lead to different changes in *in situ* density.

There is an exception for this rule. If a constant salinity contour on an ADS passes the origin; by definition, $\rho(\Theta_0, S_0, p)=\rho[\Theta(\lambda, \theta, p, t), S_0, p]$; thus, potential temperature along this contour should be constant. As a result, all water parcels on this contour can exchange their positions. Furthermore, all ADSs starting from points on this contour are the same.

If one wants to know where water parcels A and B can travel to through adiabatic movements, one should plot the corresponding ADS for these water parcels, shown as $\sigma_{a, A}$ and $\sigma_{a, B}$ in Fig. 1b. It is clear that these two ADS would not pass through point O in general.

Similar to the ADS, the PDS is defined station by station, so that its definition is independent of the path or the sequence used to define it. By definition, all water parcels sitting on a PDS can adiabatically travel to the reference pressure level, such as point O. However, water parcel O cannot travel to point A and B through adiabatic motions without leaving this PDS. Furthermore, water parcels A and B cannot exchange their positions freely, as marked by the small crosses in Fig. 2a. This non-communication property of the PDS is again due to the nonlinearly of the equation of state of seawater. As a result, water parcels on a PDS cannot travel adiabatically along the surface (except the central point O) without altering the shape of the PDS. Therefore, PDS is not a surface for adiabatic movement of water parcels.
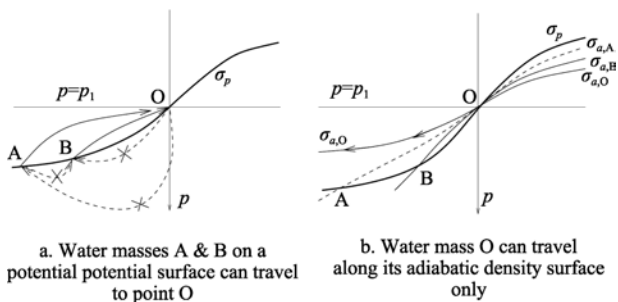

a. Water masses A & B on a potential potential surface can travel to point O

b. Water mass O can travel along its adiabatic density surface only

Fig. 2   The property of the PDS. The dashed lines with arrow and crosses in (a) indicate forbidden paths; $\sigma_{a, O}$, $\sigma_{a, A}$ and $\sigma_{a, B}$ in (b) indicate the ADS starting from point O, A and B. respectively. See the main text for detailed discussion

There are special lines on the PDS. First, a constant salinity contour on a PDS is also a constant potential temperature contour. By definition, all parcels on a PDS should have the same density when they arrive at the reference pressure. Thus, if parcels 1 and 2 have the same salinity, because $\rho(\Theta_1, S_0, p_r)=\rho(\Theta_2, S_0, p_r)$, their potential temperature should be the same; thus, all water parcels on a PDS that are also on the same S-contour or Θ-contour are interchangeable.

A close examination reveals that for a PDS, point O lies on the ADSs started from all points on this surface, as depicted by the solid arrows in Figure 2b. However, the ADS starting from point O does not pass through these points, as indicated by the solid line with an arrow in Figure 2b. Therefore, the PDS is a not a neutrally buoyant surface for water parcel O.

2.2   The neutral density surface and its link with the adiabatic density surface

The NDS (or neutral surface) has been defined as following: "Neutral surfaces are defined so that small isentropic and adiabatic displacements of a fluid parcel on a neutral surface do not produce a buoyancy restoring force on the parcel." (McDougall, 1987a); "A neutral trajectory is a three-dimensional path in the ocean, and is defined such that no buoyancy forces act on a water parcel when it is moved a small distance along this path." (Eden, et al, 1999); "…, so-called neutral surfaces have been introduced. They are defined so that a water parcel that is displaced adiabatically along a neutral surface always has the same density as the surrounding water, and is therefore in vertical equilibrium" (Nycander, 2011).

A concise definition of the NDS is as follows: at any point on this surface its tangent surface is coincident with the tangent of the potential density using the local pressure as the reference pressure. However, due to helicity, such a surface does not exist in the world ocean.

By definition, the ADS and the PDS are different from the NDS. Since the definition of the NDS is related to the tangent surface at each point, a point on a NDS is closely related to water properties of other stations in its vicinity. On the other hand, both the ADS and the PDS are defined point by point; thus, in theory the vertical position of a point on a ADS or PDS is solely determined by water properties

at this station, and it is not directly linked to water properties of other stations in its vicinity, if we omit the dynamical connection of water masses at adjacent stations through lateral mixing.

The neutral density and NDS have been widely studied and used in descriptive oceanography. From the discussion above, although the NDS and some other similar surfaces can be used to represent the mixing surface approximately, these surfaces are not exactly the surface for the mixing paths. In fact, up till now, to the best of my knowledge, we have been unable to identify any surface that can be claimed as the mixing surface.

3   The adiabatic density surface, potential density surface and neutral density surface

3.1   The difference between curves on these surfaces

The intersections of an ADS, PDS and NDS with a given (meridional or zonal) section in the ocean are called the Adiabatic Density Curve (ADC), Potential Density Curve (PDC) and Neutral Density Curve (NDC), respectively. In this section, we will use two pairs of stations taken from the WOA01 database to show the relation between these curves. The first pair of stations is located at (30°30′W, 51°30′S and 50°30′S) and the origin is at 1000 db (Fig. 3).   The horizontal position of this pair of station is denoted as $x=[-1, 0]$, with $x=0$ denoting the station at (30°30′W, 50°30′S).   In Fig. 3, σ_a denotes the ADC, σ_1 denotes the PDC (with 1000 db as the reference pressure), and γ denotes the NDC. All these lines start from $x=0$ to $x=-1$, with horizontal resolutions $\Delta x=1, 0.5, 0.1, 0.001$. The corresponding temperature and salinity at these new sub-stations are calculated by a simple linear interpolation from the WOA01 data.

Fig. 3   Depth difference for three types of curve for a station pair at (30°30′W, 51°30′S) and (30°30′W, 50°30′S), starting from 1000 db of the WOA01. Δx is the horizontal resolution in σ_1 or NDC γ for different horizontal resolution of Δx degrees. a. ADC σ_a; b. depth difference between σ_a and PDC

Although there are many different ways to obtain a NDC, such as the minimization technique (Eden, et al, 1999) or the neutral density code provided by Jackett, et al (1997), a straightforward way is to follow the original idea of Forster, et al (1976) and construct this set by using the simple Euler forward method, which can provide a solution with highly desirable accuracy. Starting from point 0 at 1000 db level, one can find the intersection of

the PDC σ_1 with the next substation on its southern side. Denote the corresponding intersecting pressure at this new substation as p_1. Using p_1 as the new reference pressure, a new PDC σ_{p_1} can be defined, and its intersection with the next substation on its left side can be found. In this way, a NDC γ between stations $x=0$ and $x=-1$ can be defined. The NDCs obtained vary with the resolution.

By definition, when $\Delta x=1$, σ_1 and γ are identical.

As a result, the dot-dashed and heavy curves are coincident in Fig. 3b. The end points of both σ_1 and σ_a are independent of the horizontal resolution; thus, the end points of σ_a–σ_1 at station x=−1 are independent of horizontal resolution. On the other hand, the NDCs gradually change with increasing horizontal resolution, as does the shape of the heavy curves denoting σ_a–γ. Since the accuracy of the simple Euler forward method has an error of O(Δx), the NDCs gradually converge to a limiting curve as resolution becomes finer. In fact, a resolution of Δx=0.001 (Δx=111 m, in dimensional coordinates) is quite adequate.

In this case, both σ_1 and γ are shallower than σ_a. However, this is not true in general. Fig. 4 shows the situation with another station pair taken at (149°30′E, 19°30′N and 20°30′N) from the WOA01. It is clear that at this location, both σ_1 and γ are deeper than σ_a.

3.2 The difference between the potenial density surface and adiabatic density surface

The next step is to compare a pair of ADS and PDS starting from the middle of the subtropical gyre in the North Atlantic Ocean at depth of 1000 db, Fig. 5. Although these two surfaces look quite similar to each other, their difference can be quite large, on the order of 200 db. As shown in Fig. 5b,
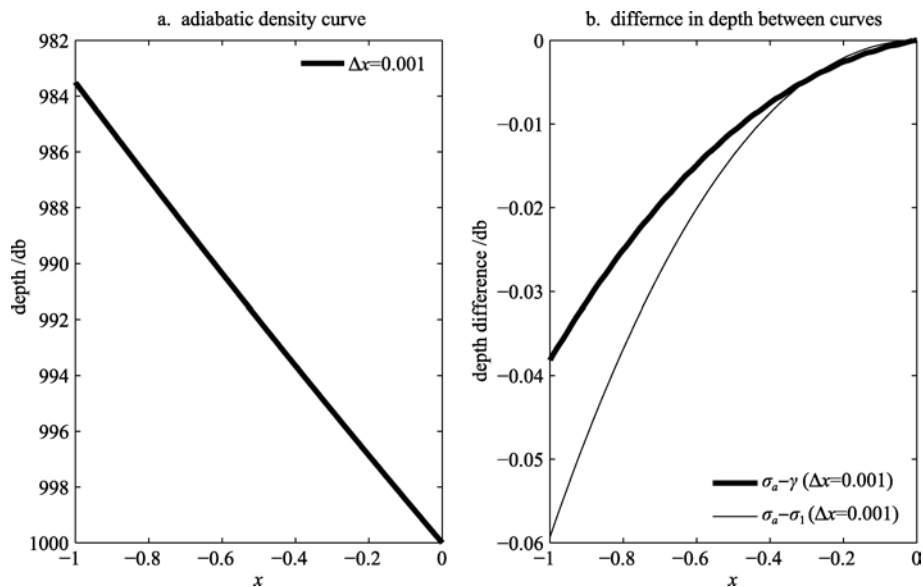

Fig. 4 Depth difference for three types of curves for a station pair at (149°30′E, 19°30′N and (149°30′E, 20°30′N), starting from 1000 db of the WOA01. Δx=0.001° is the horizontal resolution. a. ADC σ_a; b. depth difference between σ_a and PDC σ_1 or NDC γ
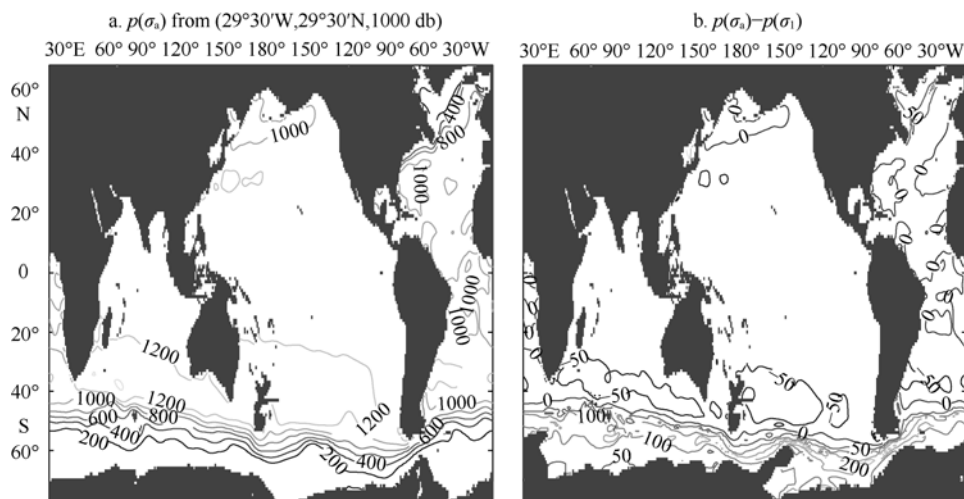

Fig. 5 a. Depth of the ADS for a water parcel originated from (29°30′W, 38°30′N, 1000 db), units: db; b. depth difference, $p(\sigma_a)$–$p(\sigma_1)$, units: db
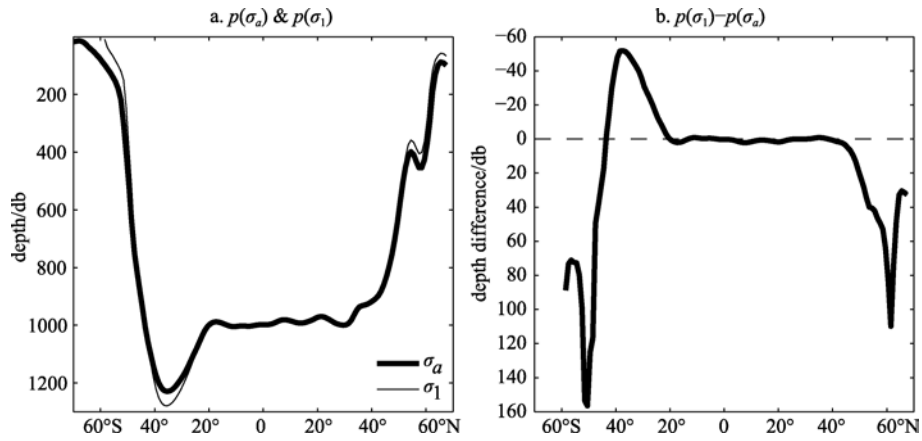
Fig. 6   Depth of the ADC and the PDC for a water parcel originated from (29°30′W, 38°30′N, 1000 db) in the North Atlantic Ocean

there is a major difference between these surfaces in the Southern Ocean, especially near the core of the Antarctic Circumpolar Current. We examine the details of this difference by taking a meridional section along the 29°30′W, Fig. 6. In this section, the ADS is shallower than the PDS at middle and low latitudes; however, the ADS is deeper than the PDS at high latitudes.

As discussed above, water parcels on an ADS cannot exchange their positions on the same ADS during adiabatic movements (except for the trivial cases of equal potential temperature and salinity). This point is illustrated clearly by plotting the ADCs for water parcels lying on the same ADC. Fig. 7a shows the ADCs starting from different latitudinal positions south of 38°30′N (the origin of this ADC). It is clear that all these new ADCs do not pass through the 38.5N station at the same depth (1000 db). Instead, the

first two new ADCs pass through the 38°30′N station at shallower pressure levels, indicated by the negative values. On the other hand, the new ADCs starting from more southward locations pass through the 38°30′N station at pressure levels deeper than 1000 db. This set of ADCs confirms the conceptual drawing shown in Fig. 1b, including the cases of passing through point O above and below.

Similarly, water parcels on a PDS cannot exchange their positions on the same PDS through adiabatic movements. This point can be illustrated clearly by plotting the ADCs for water parcels lying on the same PDC. Fig. 7b shows the ADCs starting from different latitudinal positions south of 38°30′N, the origin of this PDC. It is clear that all these new ADCs pass through the 38°30′N station at the same depth (1000 db). However, between their starting latitude and the 38°30′N station, the new ADCs
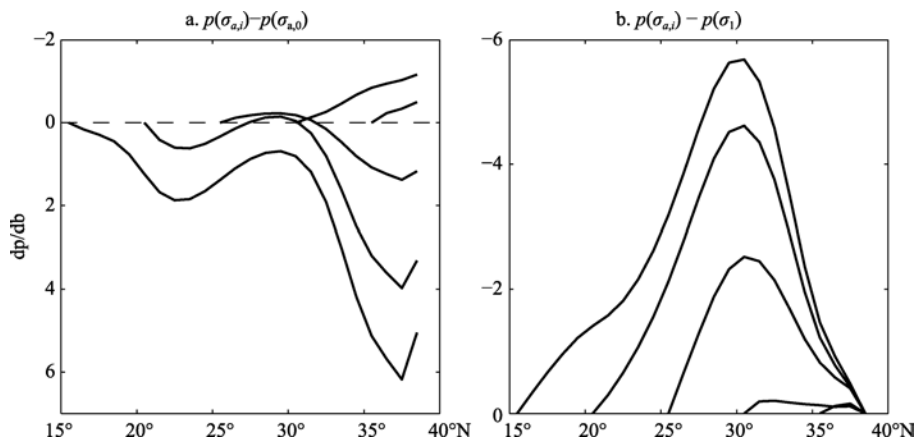

Fig. 7   a. Difference in depth of the ADCs for water parcels along the ADC started from (29°30′W, 38°30′N, 1000 db) in the North Atlantic Ocean. Note that pressure difference is positive for the lower part of the figure, indicating the new ADS is deeper than the one starting from 38°30′N. b. Difference in depth of the ADCs for water parcels taken along the PDC started from (29°30′W, 38°30′N, 1000 db) in the North Atlantic Ocean

starting from stations south of 38°30′N are shallower than the PDC, as shown in Fig. 7b by the negative pressure difference. This set of ADCs confirms the schematic drawing in Fig. 2b.

3.3   Application to the WOCE P-15 section

As the next example, we show the comparison between four different types of surfaces based on

the high-accuracy hydrographic data collected on the WOCE P-15 section, which is approximately along 179°30′W in the Pacific Ocean. Fig. 8a shows four curves, including an ADC, a PDC, a potential temperature curve and a NDC (constructed by Euler method discussed above), all starting from 41°29′24″N at a depth of 1000 db.
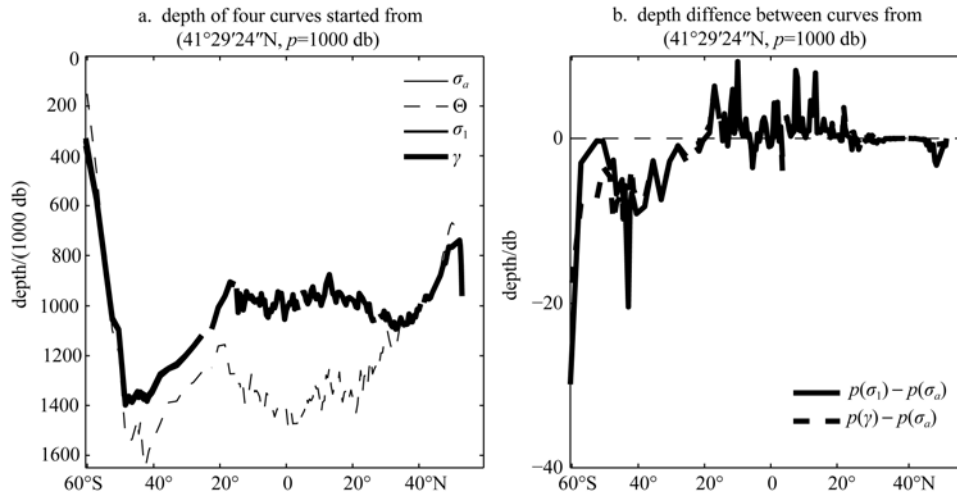

Fig. 8   a. Depth of different curves along 179°30′W section started from (41°29′24″N, 1000 db); b. depth difference between curves started from (41°29′24″N, 1000 db)

It is clear that a potential temperature surface is quite different from the other three surfaces (they overlap each other in this map). Since the potential temperature surface is very close to that of entropy surface, the entropy surface is also quite different from the other three surfaces.

A close examination of these other three surfaces is shown in Fig. 8b. For this section, the difference between the ADC and the NDC is approximately the same as that between the ADC and the PDC. The differences are within 10 db most of the time, and the PDC is slightly closer to the ADC than the NDC.

3.4   The intrinsic difference between the PDS and the ADS

As shown above, the difference between the PDS and the ADS is on the order of tens of db. On the other hand, due to climate variability, water properties in the ocean can vary greatly. For example, Joyce, et al (2000) reported that the annual-averaged subtropical mode water potential vorticity at 200 m depth can vary over the range of $4\times10^{-11}\sim12\times10^{-11}$ m^{-1}·s^{-1}. Deser, et al (1996) showed that the temperature

anomaly in the upper ocean is on the order of one degree and the variability of the 9℃ isothermal depth is on the order of 40 m. Therefore, the depth differences between the PDS, the ADS and the NDS are on the same order as the climate variability in the ocean. Are these differences still meaningful? As will be shown shortly, the difference between the PDS and the ADS is an intrinsic property entirely due to the thermobaricity of seawater.

As an example, we calculated property difference along a PDC starting from (170°30′W, 40°30′N, 500 db) using WOA01 data. Moving southward along this curve, water becomes warm and salty, and the compressibility is gradually reduced, Fig. 9a. This PDC ($\sigma_{0.5}$) becomes deeper in the subtropical gyres in both hemisphere, but it is slightly shallower in the equatorial band, Fig. 9b. Due to differences in compressibility and pressure, a water parcel originating at θ_0=40.5° and moving southward along this PDC should gradually change its density; the *in-situ* density change during adiabatic motions is $\triangle\rho=\rho_0\triangle k_\eta\triangle p$, where $\rho_0 \approx 1030$ kg·m^{-3} is the mean reference density, $\triangle k_\eta = k_\eta(\theta)-k_\eta(\theta_0)$ and $\triangle p=$

$p(\theta)$–$p(\theta_0)$ are the difference in compressibility and pressure between the stations at latitude θ and θ_0. By definition, when a water parcel at station θ adiabatically arrives at θ_0, it should have the same *in situ* density as the local parcel. However, when the parcel from the starting latitude θ_0 adiabatically moves to station θ, its *in situ* density is different from the local parcel; the corresponding density increment is $\triangle\rho=\triangle k_\eta\triangle p$. If $\triangle\rho>0$, in order to have a density

equal to the local water mass, the parcel originating at θ_0 must move upward toward an environment with lower pressure; thus, the equivalent depth of the ADS (σ_a) must be shallower than $\sigma_{0.5}$ at this station θ, indicated by a negative value of $p(\sigma_a)$–$p(\sigma_{0.5})$ in Figure 9f. A rough estimate of this depth difference can be calculated as $\delta p \approx - g^2\triangle\rho/N^2$, where N^2 is the buoyancy frequency. The exact value can be calculated from solving Eq. (1).
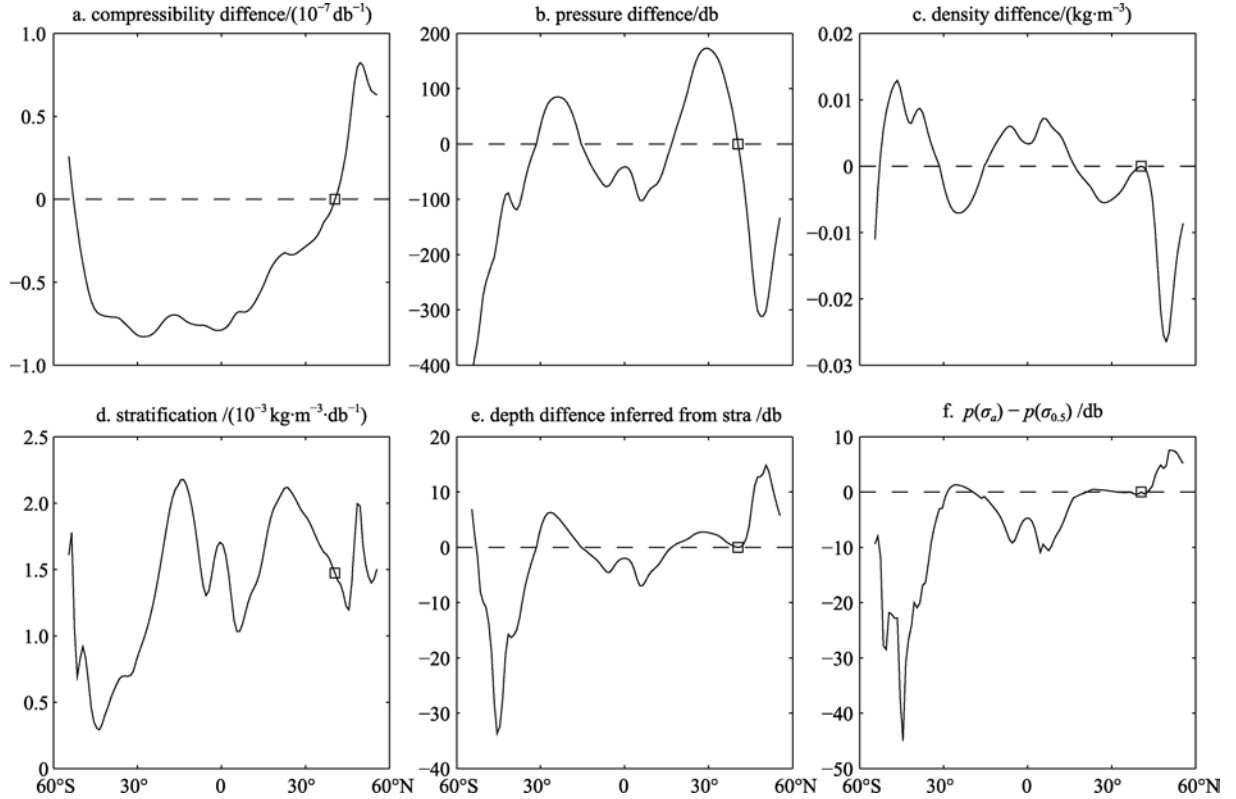

Fig. 9 Properties changes along a PDC on the 170°30′W section starting from (40°30′N, 500 db), as marked by the square in each panel) based on the WOA01. See the main text for detail

4 Multiplicity of the adiabatic density surface

Due to the nonlinearity of the equation of state, NDS can have multiplicity, or the so-called helicity (Jackett, et al, 1997). It is also well known that in many places the PDS can have multiple sheets (or reversion). A classical example is that at lower latitudes in the Atlantic Ocean, potential density σ_0 (using sea surface as the reference) seems unstable below 3000 db. This unstable feature can be interpreted as a sign of multiple sheets of PDSs. This seemingly unstable stratification disappears, if we plot potential density maps using deeper pressure levels, such as 2000 db, as the reference pressure.

The nonlinearity of the equation of state also affects the distribution of ADSs, giving rise to multiple sheets of ADS. As an example, we show the case with the original water parcel taken from (30°30′W, 75°30′S, 0 db), Fig. 10. This water parcel may be used as a rough representative of the source of AABW formed in the Weddell Sea. The corresponding ADS has two branches. The upper branch is at the 1500 db level, and the lower branch is about 1500 db deeper, Fig. 10.

To demonstrate the detailed structure of these surfaces we include a meridional section along 30°30′W, Fig. 11a. Three curves represent intersections of different surfaces (starting from 75°30′S

and 0 db): the PDC (σ_0), the NDC (γ) and the ADC (σ_a). The NDC is calculated by using a simple Euler forward method. The NDCs obtained using the simple Euler method with horizontal resolution of 1 degree and 0.1 degree are virtually the same, suggesting good numerical convergence.
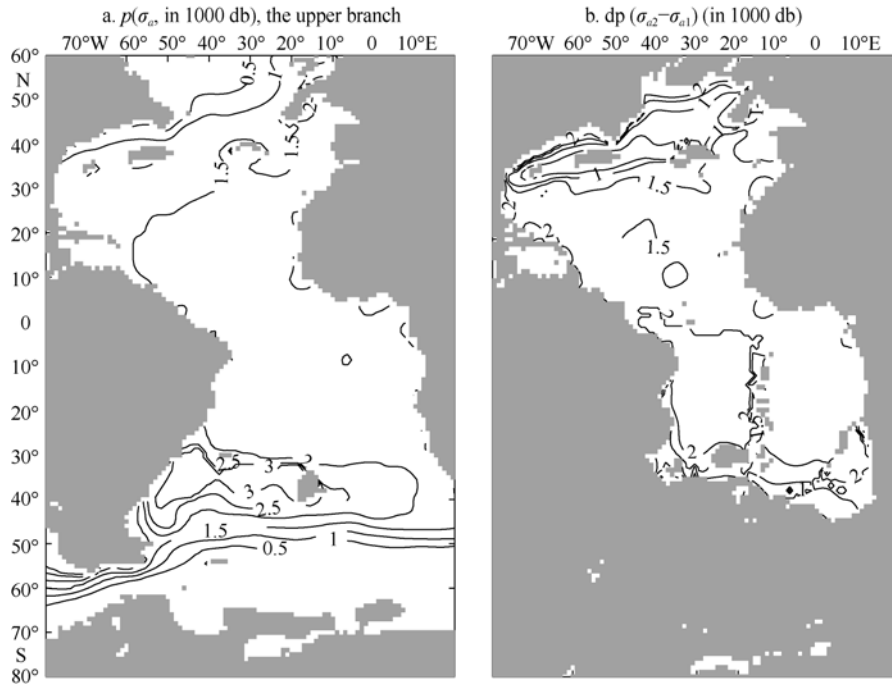

Fig. 10   a. An ADS map for the Atlantic sector (depth in db), starting from the sea surface at a station (30°30′W, 75°30′S), as marked by a star near the southern boundary; b. the depth difference between the lower and upper branches of this ADS
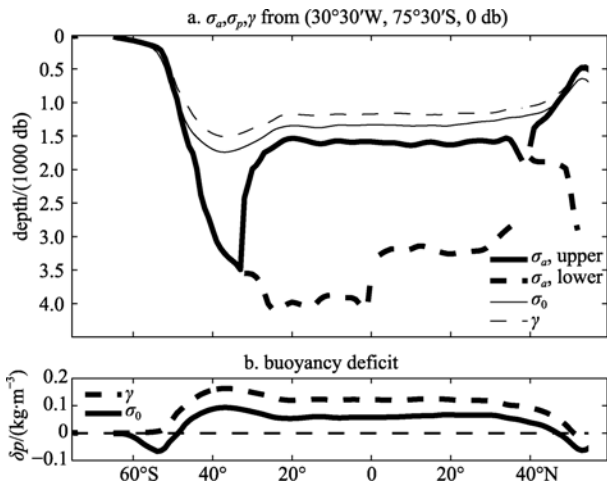

Fig. 11   A meridional section along 30°30′W. (a): Intersections with four surfaces, all started from the sea surface at station (30°30′W, 75°30′S); (b): buoyancy deficit along the NDC and the PDC

As shown in Fig. 11a, the differences between these curves are rather small in the latitude band south of 50°S; however, their differences grow rapidly north of 50°S. The most interesting feature is the bifurcation of the ADC at (32°30′S, 3,495 db), i.e. the multiple solutions of Eq. (1). The upper branch quickly rises to the 1600 db level; while the

lower branch sinks to the 4000 db level. Thus, in a rather crude way, the upper branch of the ADC is linked to the formation of the Antarctic Intermediate Water (AAIW) with a core depth around 1.5 km; the lower branch of the ADC is linked to the AABW formation. However, one should recall that the WOA01 data were obtained after much data manipulation, including interpolation, extrapolation and smoothing; thus, the ADC and NDC calculated from such a climatological dataset may not accurately represent the actual *in situ* observations at any one time. Nevertheless, the bifurcation of ADC in this section is a good example of the multiplicity of ADS.

The density difference between the original water parcel and the local parcel along a NDC and a PDC are plotted in Fig. 11b, where positive value of buoyancy deficit indicates that the original parcel is heavier than the local parcel. It is clear that both PDC and NDC are not buoyancy-free, i.e., not neutral.

Further comparison of these curves can be carried out via sea water property distributions along this section. As shown in Fig. 12a, if we use potential

temperature as a tracer to keep track of the water mass trajectory, the lower branch of the ADC seems to be a better choice; while the upper branch of the ADC and the NDC also seem to follow certain secondary tongue-like features. On the other hand, if we use salinity as the tracer to track the water mass, there are some quite interesting results, Fig. 12b. First, south of 35°S, the NDC seems to trace the shallow salinity minimum contours; however, north of 35°S, the NDC moves across salinity contours. One interesting point is that the bifurcation of the ADC around 30°S seems to be closely related to the intrusion of the high salinity tongue from the North Atlantic Ocean. We speculate that in this part of the 30°30′W section, the shape of the ADC (including its bifurcation) may be primarily controlled by salinity.
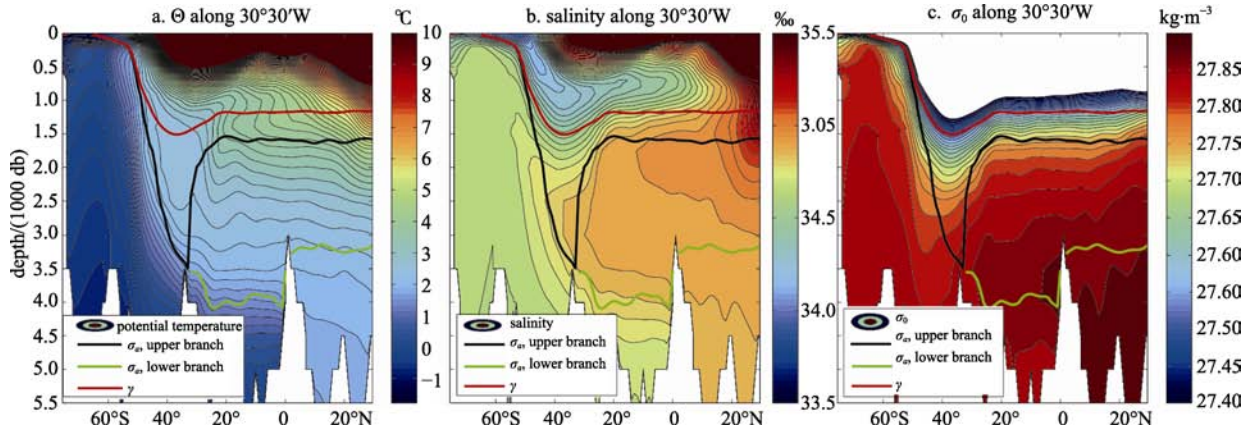

Fig. 12   Section along 30°30′W of a. potential temperature; b. salinity and c. PDS (σ_0), including a NDC and two ADCs taken from Fig. 11

The existence of the high salinity tongue in the deep ocean at this latitude band is clearly related to the bifurcation of the PDC in the vicinity, Fig. 12c. The bifurcation of the σ_0 contours in the deep part of the Atlantic Ocean is a well-known phenomenon. For a long time, such a feature has been viewed as a disadvantage of the potential density function. Indeed, if one uses potential density as the indicator of the local stratification away from the reference pressure, such artificial unstable stratification may appear in the potential density section map. However, such a bifurcation is not entirely meaningless. As shown above, the bifurcation of the potential density at this depth is closely related to the high salinity tongue in the ocean. Furthermore, such a tongue-like feature in both salinity and potential density section may be related to the potential mixing paths in the ocean. As we will argue shortly, there are many potential mixing paths in the turbulent ocean, so that all of these curves may have its own specific meaning.

Note that these curves represent quite different trajectories (or paths) in the ocean. As shown in Fig.

13, the large black dots on the low-left corner of each panel depict the initial position and properties of the water parcel. The black (red) curves depict the position and water mass properties along the upper (lower) branch of the ADC. By definition, although the water parcel travels along an ADC for a great distance, its potential temperature and salinity remain unchanged; however, its *in-situ* density should be the same as the local water mass, black and red curves in Fig. 13c.

In contrast, the imaginary water parcel following the NDC adapts new Θ-S properties at each station, as shown by the blue curves in Fig. 13. In addition, *in situ* density of the parcel traveling along the NDC does not match that of the local parcel, as shown in Fig. 11b. Strictly speaking, this imaginary water parcel has lost its own identify each time it passes through a new station. Thus, the NDC is not a material trajectory.

5   Mixing paths

The mixing path is the trajectory of a water mass spreading/ transforming in the ocean. Many

attempts have been made to find mixing paths in the ocean. For example, when cold and dense water is formed along the edge of Weddell Sea, it moves down into the open ocean, mixing with the ambient water on its way. Some early work may have used a PDS to trace the mixing paths; however, it was soon realized that the PDS is not the suitable surface.

Forster, et al (1976) postulated an improved way for identifying the mixing path, as illustrated in Fig. 14. The basic idea of Forster, et al (1976) seems to provide the physical background of the NDS developed by McDougall and others, e.g. McDougall (1987a), Jackett, et al (1997), Eden, et al (1999).
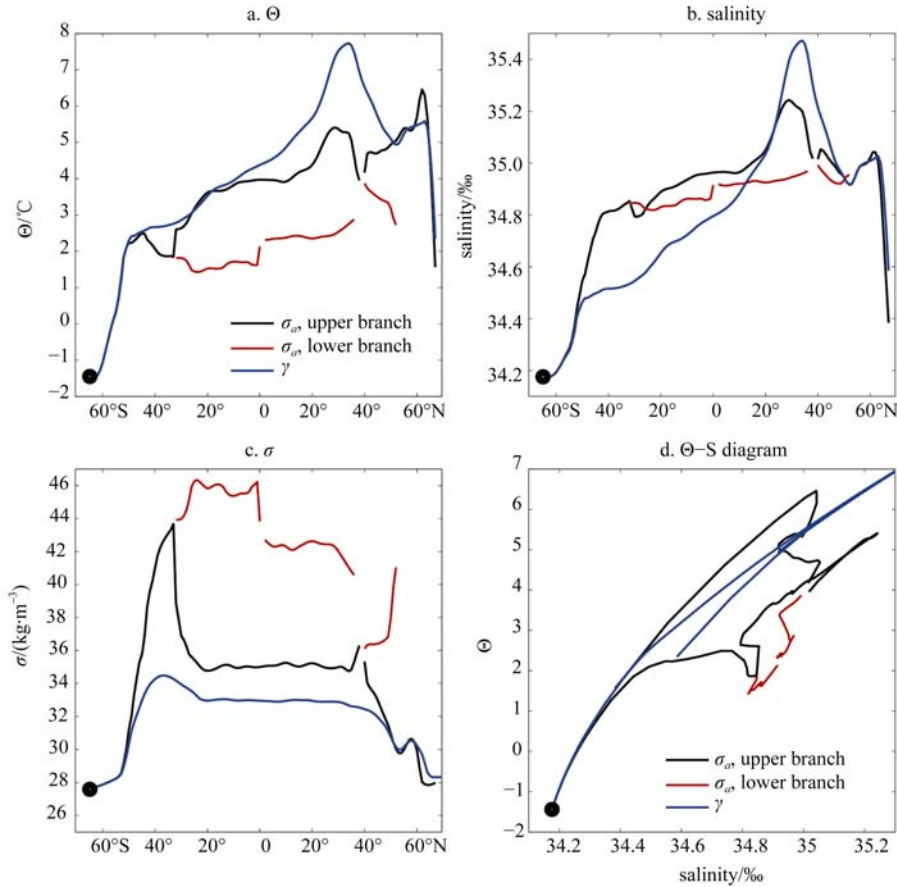

Fig. 13   Property distribution along different curves: the upper (black) and lower (red) branches of the ADC, and the NDC (blue). The black dot at the lower-left corner of each panel indicates the initial position and property of the water parcel at the beginning of the trajectory
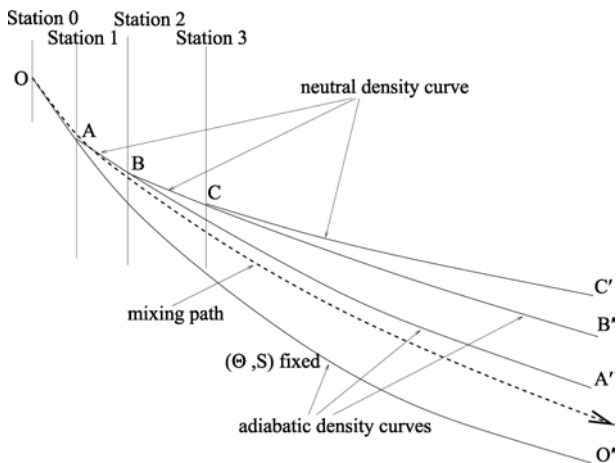

Fig. 14   A sketch illustrating the relation between the ADC, the NDC and the mixing path

Assume a source of deepwater is located at depth O at station 0 and we want to trace its mixing path. First, we trace water parcel O adiabatically to station 1, where it sinks (or rises) to a level where its *in situ* density is equal to that of a parcel A. The first segment of the mixing path is marked by the solid line OA. Starting from A, Forster and Carmack (1976) suggested using parcel A, instead of parcel O, to trace the mixing path. Once again, parcel A is moved adiabatically to a new rest level at the next station so that its new *in situ* density is the same as that of parcel B. Thus, the second segment of the mixing path, line AB, is determined. By repeatedly

using the same procedure, the whole mixing path is determined.

In light of the ADS defined in this study, it is clear that the first segment of the mixing path defined above is coincident with the ADC starting from point O, as depicted by the solid line OAO' in Fig. 14. The second segment of the mixing path defined above is coincident with the ADC starting from point A, as depicted by the thick line ABA'. Similarly, the third segment of the mixing path is coincident with the ADC starting from point B, as depicted by the thin black line BCB'.

A path defined in this way is not a mixing path. In fact, during the first segment of the path, the original water parcel O should mix with the ambient water. Due to cabbeling, a nonlinear effect of the equation of state, mixing always produces a new type of water whose density is greater than the mean density of the parental water masses. Hence, the mixing path is different from curve OCC' found through the search process discussed above. It is, thus, obvious that the true mixing path is quite different from what postulated by Forster, et al(1976). To mark this difference, we use a heavy dashed line with arrow in the lower-middle part of Fig. 14 to depict the real mixing path.

In the present case, source water from the edge of Antarctica is cold and relatively fresh, and its new environment is slightly warmer and saltier. Thus, mixing makes the water mass tend to be slightly lighter than the original water mass, but slightly heavier than that of the environment; thus, in this schematic figure, we plot the dashed curve between the ADC and NDC.

6　Reexamining mixing paths

A close examination reveals that the NDC and the ADC shown in Fig. 11a represent two extreme limits for mixing in the ocean.　In a turbulent ocean full of eddies of different sizes and other chaotic motions the number of potential trajectories of a parcel is infinite, Fig. 15. Assuming water parcel A is within the water column AA, there are many potential paths for this water parcel to travel from column AA to column BB, and arriving at different depths.
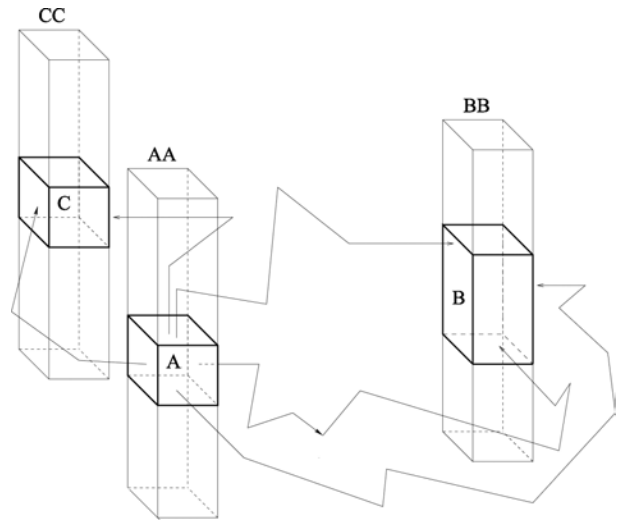

Fig. 15　Potential trajectories for water parcels travelling in a turbulent ocean

Furthermore, water properties in water column BB are controlled by complicated processes. As for a water parcel B within this column, turbulent motions bring information from all sides of this grid box; thus, one should not assume *a priori* that information from a specific trajectory can completely dominate the concentration at this grid box.

In the following analysis we will assume that the water parcel of interest can be treated as aninfinitely small parcel, i.e. when it travels to station 1 in Fig. 14, it will not affect the background concentration. Here, we introduce a mixing ratio m, which is defined as follows. Assume that at station 0, tracer concentration of the parcel is C_0. We will idealize the continuous process of mixing along the trajectory in finite difference as follows. To begin with, we divide the continuous trajectory into a set of stations with finite distance between them. Assume the parcel conserves its tracer during its movement between stations. As it arrives at a new station, it mixes with the new local environment C_{ref} according to the following relation

$$C_1 = mC_{\text{ref}} + (1-m)C_0 \qquad (2)$$

Therefore, $m=0$ is the case with no mixing. As such, the water parcel conserves its original identity in both potential temperature and salinity. The trajectory of such a water parcel corresponds to the ADC in Fig. 16.

The case with $m=1$ corresponds to the NDC in Fig. 16. In this case, at each station the water parcel
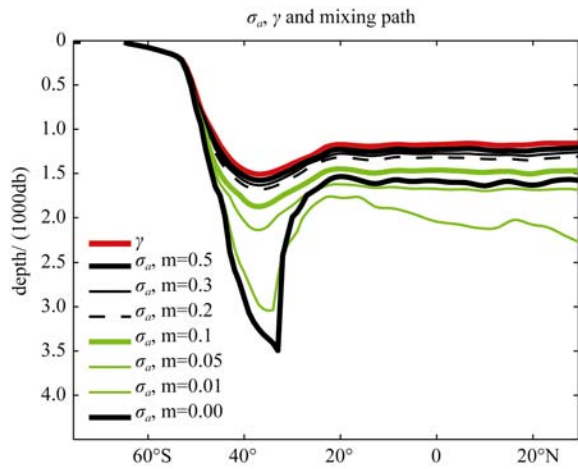
Fig. 16   Mixing trajectories with different mixing ratio through the 30°30′Wsection

takes up the new local properties and continues to move on. In a strict sense, the corresponding trajectory does not represent a trajectory of a water parcel because the original information carried by a water parcel is completely lost each time when it arrives at a new station. In fact, this curve is the envelope of infinitesimal trajectory segments belonging to all infinitesimal water parcels selected along this curve.

In general, $0<m<1$, and the corresponding trajectories are shown in Fig. 16. By definition, during the transition from one station to the next, a

water parcel conserves its properties and each segment is an ADC; when it arrives at the next station, its *in situ* density is the same as the local water mass. However, through mixing it acquires the partially new potential temperature and salinity. Due to cabbeling, the transformed water parcel has a density slightly greater than the mean density of the parent parcels.

As shown in Fig. 17a, water parcel A moves adiabatically and arrives at a new station at the same pressure level as parcel B. By definition, parcels A and B sit on same *in situ* density contour, although they may have different potential temperature and salinity in general. For simplicity, we assume that the mixing ratio is roughly 0.5. As a result, a new parcel C is produced. Due to cabbeling, this new parcel's *in situ* density is larger than both parcels A and B, and it should sink to a slightly deeper level.

Similarly, when parcel C moves to the next station, it should sit on the same pressure level with the local parcel D that has the same *in situ* density. Through mixing, the newly formed parcel E is slightly heavier than both parcels C and D, and thus sinks to a deeper level.
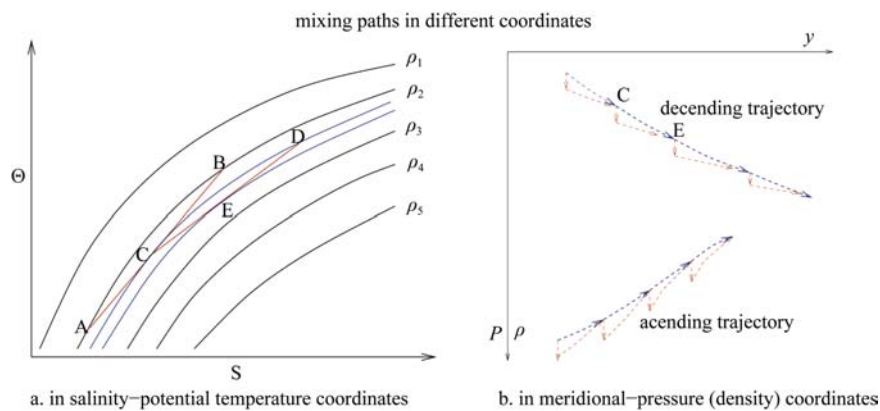

Fig. 17   Sketches of mixing paths in the phase space and a meridional section. a. Cabbeling in the theta-S diagram; b. mixing paths in the meridional-pressure coordinates

Therefore, for the general case $0<m<1$, cabbeling takes place each time there is mixing between water parcels with same *in situ* density, but different potential temperature and salinity. Although mixing processes in the ocean may take place in different forms, either continuously or episodically, we can still conceptually separate them into segments, as

illustrated in Fig. 17b.

For example, the case when the mixing trajectory moves gradually to deeper levels is illustrated in the upper part of Figure 17b. After mixing, the new water parcel C should have a slightly greater density and thus sink to a deeper level, red arrow below point C. The actual path

from point C to the next point E remains unclear because in a turbulent ocean, the passage of individual water parcels cannot be well-defined and may be subject to chaotic and random motions. Such uncertainty of the detailed passage between two stations is indicated by the potential sub-trajectories marked by dashed red arrows or dashed blue arrows. The corresponding case of an ascending trajectory in the meridional section is illustrated by the sketch in the lower part of Fig. 17b.

With the effect of cabbeling in mind, we now return to Fig. 16. Curves corresponding to $m=0$ and $m=1$ have been discussed above. In fact, it has been noticed that when mixing takes place, the resulting water parcels should acquire slightly higher density and thus tend to leave the NDS. Although the NDS may be used as the base of potential mixing of two water parcels at infinitesimal distance on this surface, mixing paths do not lie on such a surface; i.e. in the case of $m=1$, the curve does not represent a trajectory for a single parcel. In the other extreme case of $m=0$, there is no mixing, and the trajectory is an ADC, which is different from a NDC.

For the general case $0<m<1$, at each new station a water parcel acquires a new potential temperature and salinity. Due to cabbeling this newly formed water parcel tends to sink to a slightly deeper level, and curves in Fig. 16 with $0<m<1$ do include such physical processes.

Density increase due to cabbeling can be calculated as

$$\Delta \rho_{cabb} = \rho\left(S_{mix},\Theta_{mix},p_{mix}\right) - \rho\left(S_0,\Theta_0,p_{mix}\right)$$
$$\simeq \rho_0\left[-\alpha\left(\Theta_{mix}-\Theta_0\right)+\beta\left(S_{mix}-S_0\right)\right] \quad (3)$$

where Θ_0, Θ_{mix}, S_0, and S_{mix} are the potential temperature and salinity of water parcel before and after mixing, p_{mix} is the *in-situ* pressure, and $\rho_0 = 1030$ kg·m^{-3} is the constant reference density, α and β are the thermal expansion coefficient and saline contraction coefficient. Each station the *in situ* density increase due to cabbeling is on the order of 10^{-3} kg·m^{-3}, and the accumulated change in density is on the order of 50×10^{-3} kg·m^{-3}; such density changes are not negligible. In addition, the density change due to cabbeling is large for a small

mixing ratio. By definition of the NDC, there is no cabbeling for the case with $m=1$ because original information is completely lost at each station.

Due to the increase in density after mixing, a water parcel should sink to a slightly deeper level, and the corresponding change in the pressure level is calculated as

$$\Delta p = \Delta \rho_{cabb}\left(\frac{\partial \rho_\theta}{\partial p}\right)^{-1}, \text{ where } \partial \rho_\theta / \partial p \text{ is the local}$$

stratification (in pressure coordinates). In the present example, the adjustment of the pressure level due to cabbeling is small, on the order of a few tenths of db. Over the distance from 60°S to the equator, the total accumulation of sinking due to cabbeling is on the order of 10 db (for the case with small mixing ratio) or less (for the case with large mixing ratio). Such pressure adjustment is much smaller than that associated with the vertical movement between stations. Nevertheless, depth adjustment due to cabbeling is not negligible, and is an essential and important part of the physical processes taking place along the trajectories.

This sinking process may be accomplished during the transition from one station to the next; but, the exact passage from one station to the next is not resolved within this truncated version of mixing in the ocean. However, an important point is that the trajectories shown in Fig. 16 with $0<m<1$ can be treated as some realistic trajectory, which includes the effect of cabbeling; hence, we may use such trajectories as a tool in the study of a mixing path in the ocean.

In order to trace the mixing trajectory, one can follow two steps: first, decide on the horizontal projection of the potential trajectory; second, choose the suitable mixing ratio. At this time, we do not have a clear-cut way for carrying out these steps; however, in the following analysis we will look at the mixing ratio anyhow.

McDougall (1987b) identified the ADS as the surface on which the so-called SCV (Submesoscale Coherent Vortices) move around in the world oceans. Ideally, SCVs conserve all their properties, so that they move on an ADS. However, the ocean is turbulent, with eddies of different sizes and

properties. Thus, mixing takes place in the ocean through all spatial and temporal dimensions. In particular, the meso-scale eddies have a scale on the order of 100 km or less, and the submesoscale eddies, including SCVs, have a scale on the order of 1~10 km. There are all sorts of eddies with scale smaller than 1 km, all the way down to the Kolmogorov scale, which is on the order of 1 mm and it is the scale at which   molecular dissipation operates.

Mixing in the turbulent oceans is realizedized through mixing carried out by these eddies. In this sense, the propagation and transformation of water masses   in the ocean can be visualized as a cloud of eddies, very much like the cloud demonstrated in the classical laboratory experiment by Stommel, et al (1958). Such a cloud of eddies can be best seen through the tracer release experiments carried out by Ledwell, et al (1993, 2000). A recent study based on Lagrangian subsurface drifters   and an eddy-resolving numerical model (Bower, et al, 2009) also showed that a major portion of water masses associated with the deep branch of the meridional overturning circulation in the North Atlantic is transported southward by eddies through the mid ocean, instead of the narrow deep western boundary current discussed in many previous studies.

7   Final remarks

We have reexamined the relations between the ADS, PDS and NDS in detail. The concept of ADS is very useful in analyzing gravitational potential energy related to lateral eddy diffusion in the ocean, as discussed by Huang (2014). The application of the ADS and the NDS represent two extreme limits of mixing paths in the ocean. In order to find out the potential mixing paths, a mixing ratio is introduced, which can take a value between 0 and 1. A close examination of these surfaces and the mixing paths defined by $0<m<1$ may provide useful information in diagnosing mixing processes and water mass formation/transformation associated with thermohaline circulation. Our discussion here is limited to examples selected from a few selected meridional sections. We emphasize that potential mixing paths in the ocean may be quite complicated and much different from those confined to such simplified meridional sections. Of course, one should not take any potential pathways as an indicator of quasi-steady flows in the ocean. One of the best illustrations of this point is the tongue-like feature associated with the Mediterranean water outflow in the North Atlantic Ocean. It is well-known that this high salinity feature is produced primarily due to the westward drifting submesoscale eddies. In view of the turbulent nature of the oceanic circulation, most quasi-steady currents studied in the previous literature should be interpreted in terms of some temporal and spatial average of eddies. There can be multiple instantaneous paths or mixing trajectories.

As we are entering the era of eddy-resolving ocean study, the examination of potential mixing paths in the ocean remains of great interest. As discussed above, however, identification of the multiple paths is a grand challenge we are facing, and further study along this line will remain stimulating into the future.

Reference

ARMI L, HEBERT D, OAKEY N, et al. 1989. Two years in the life of a Mediterranean Salt Lens[J]. J Phys Oceanogr, 19: 354–370.

BOWER A S, LOZIER M S, GARY S F, et al. 2009. Interior pathways of the North Atlantic meridional overturning circulation[J]. Nature, 459: 243–248. doi:10.1038.

CONKRIGHT M E, LOCARNINI R A, GARCIA H E, et al. 2002. World Ocean Atlas 2001: Objective Analysis, Data Statistics, and Figures[R/CD]. National Oceanographic Data Center, Silver Spring, MD: 1–17.

DE SZOEKE R A, SPRINGER S R. 2005. The all-Atlantic temperature–salinity–pressure relation and patched potential density[J]. J Mar Res, 63: 59–93.

DE SZOEKE R A, SPRINGER S R. 2009. The materiality and neutrality of neutral density and orthobaric density[J]. J Phys Oceanogr, 39, 2009, 1779–1799.

DESER C, ALEXANDER M A, TIMLIN M S. 1996. Upper-ocean thermal variability in the North Pacific during 1970-1991[J]. J Climate, 9: 1840–1855.

EDEN C, WILLEBRAND J. 1999. Neutral density revisited[J]. Deep-Sea Res. II, 46: 33–54.

FEISTEL R. 2003. A new extended Gibbs thermodynamic potential of seawater[J]. Progr Oceanogr, 58: 43–114.

FEISTEL R. 2005. Numerical implementation and oceanographic

application of the Gibbs thermodynamic potential of seawater[J]. Ocean Science, 1: 9–16.

FORSTER T D, CARMACK E C. 1976. Frontal zone mixing and Antarctic bottom water formation in the southern Weddell Sea[J]. Deep Sea Res, 23: 301–317.

HUANG R X. 2014. Energetics of lateral eddy diffusion/advection, Part I. Thermodynamics and energetics of vertical eddy diffusion[J]. Acta Oceanologia Sinica, 33: 1–18.

JACKETT D, MCDOUGALL T J. 1997. A neutral density variable for the world's oceans[J]. J. Phys. Oceanogr. 27: 237–263.

JOYCE T M, DESER C, SPALL M A. 2000. The relation between decadal variability of subtropical mode water and the North Atlantic Oscillation[J]. J Climate, 13: 2550–2569.

LEDWELL J R, WATSON A J, LAW C B. 1993. Evidence for slow mixing across the pycnocline from an open-ocean tracer-release experiment[J]. Nature, 364: 701–703.

LEDWELL J R, MONTGOMERY E T, POLZIN K L, et al. 2000. Evidence for enhanced mixing over rough topography in the abyssal ocean[J]. Nature, 403: 179–182.

LOZIER M S. 2010. Deconstructing the conveyor belt[J]. Science, 328: 1507. doi: 10.1126/science.1189250.

MCDOUGALL T J. 1987a. Neutral surfaces[J]. J Phys Oceanogr, 17: 1950–1964.

MCDOUGALL T J. 1987b. The vertical motion of Submesoscale coherent vorticies across neutral surfaces[J]. J Phys Oceanogr, 17: 2334–2342.

MONTGOMERY R B. 1938. Circulation in upper layers of southern North Atlantic deduced with use of isentropic analysis[J]. Papers Phys Oceanogr. Meteor, 6(2): 1–55.

NYCANDER J. 2011. Energy conversion, mixing energy and neutral surfaces with a nonlinear equation of state[J]. J Phys Oceanogr, 41: 28–41.

REID J L. 1994. On the total geostrophic transport of the North Atlantic Ocean: Flow patterns, tracers, and transports[J]. Prog Oceanogr, 33: 1–92.

SCHMITZ W J JR, MCCARTNEY M S. 1993. On the North Atlantic circulation[J]. Rev Geophys, 31: 29–49.

STEWART R H. 2009. Introduction to physical oceanography [M/OL]. (2009-03-27)[2013-11-26]. http://oceanworld.tamu.edu/home/course_book.htm.

STOMMEL H, ARONS A B, FALLER A J. 1958. Some examples of stationary planetary flow patterns in bounded basins[J]. Tellus, 10: 179–187.

WIJFFELS S E, TOOLE J M, BRYDEN H L, et al. 1996. The water masses and circulation at 10°N in the Pacific[J]. Deep-Sea Res, 43: 501–544.

WUST G. 1935. Schichtung und Zirkulation des Atlantischen Ozeans, Die Stratosphiire[M]. Wiss Ergebn Dtsch Atl Exped, 6, Part 1, 2: 180. (In English version: EMERY W J. 1972. The Stratosphere of the Atlantic Ocean[M]. New Delhi, India: Amerind: 112)